Metastable structures of cholesteric liquid crystals with negative diamagnetic anisotropy in magnetic fields

Arunava Chatterjee and D. H. Van Winkle
Department of Physics and Martech, The Florida State University, Tallahassee, Florida 32306-3016
(Received 29 June 1995; revised manuscript received 20 December 1996)

Recent studies of a negative diamagnetic anisotropy cholesteric (liquid crystalline deoxyribonucleic acid) in magnetic fields have revealed a morphology consisting of birefringent stripes superposed by a fingerprint texture. In order to understand why this morphology appears in high magnetic fields, we performed a numerical analysis of the elastic properties of the system. The solution of Euler-Lagrange equations associated with the Frank elastic energy shows that a high enough magnetic field stabilizes a splay-bend distortion which is damped out at lower magnetic fields. In addition, the solutions indicate that the cholesteric pitch is not constant in the presence of director fluctuations. [S1063-651X(97)05304-X]

PACS number(s): 61.30.−v

I. INTRODUCTION

Liquid crystals are always composed of anisotropic constituents. The (typically) molecular anisotropy leads to differences in the dielectric and diamagnetic susceptibilities along different body axes. Therefore, by a suitable choice for the direction of an aligning field, different types of symmetry breaking may be observed. In particular, cholesteric liquid crystalline deoxyribonucleic acid (lc DNA) when placed in magnetic fields tends to align perpendicular to the field direction [1,2]. The fingerprint texture is observed when the magnetic field is applied in a plane parallel to cover slip and slide. In addition, a texture comprised of birefringent stripes overlaid by fingerprint domains is observed at higher magnetic fields. Both textures are shown in Fig. 1. The fingerprint texture is typical of cholesteric materials for which the twist axis is oriented by a field.

The stripe texture shown in Fig. 1(b) is similar to one observed by Bouligand in a methoxy-benzilidene-butylaniline (MBBA) sample doped with cholesterol benzoate [3]. He studied the structure by optical microscopy and deduced the molecular orientation as a function of position. In effect, the cholesteric twist axis became tilted out of the plane of the slide and splayed on either side of the centerlines which include the defect sites. This splay of the twist axis manifests (in polarized microscopy) as the bright and dark stripes in Fig. 1(b). For example, where the sample's birefringence rotates the polarization towards the analyzer axis there is a bright stripe.

Reorientation of the twist axis in response to an applied magnetic field is the realization of a Fréedericksz transition in a cholesteric with negative diamagnetic anisotropy. This occurs for applied magnetic fields of 3.5 T and larger in cholesteric lc DNA. By numerical analysis, we have attempted to understand why the uniformly aligned cholesteric (which appears for 3.5 and 6.3 T fields) distorts into the stripe texture when the magnetic aligning field becomes large (9.4 T). By solving one-dimensional Euler-Lagrange equations derived from the Frank free energy, we find oscillatory distortions perpendicular to the field axis consistent with the stripe texture. These oscillatory distortions are stable only at high magnetic fields. They decay in short distances for smaller fields. In addition, a long wavelength mode parallel to the field characterized by a sinusoidal variation in the twist is found for solutions in that direction.

II. BACKGROUND

DNA fragments in aqueous solution form liquid crystalline phases [4]. The DNA rods are negatively charged in solution. Their interaction in the presence of counterions is dominated by screened Coulomb repulsion which has been described by an ionic double layer theory [5,6]. The solutions form cholesteric and hexagonal columnar phases. The cholesteric phase is stable between concentrations of 150 mg DNA/ml and 400 mg/ml with pitch p increasing with concentration from approximately 2 to 10 μm [7]. Relative to its helix axis, DNA has a negative diamagnetic anisotropy. The free energy is lowered by alignment of the molecule perpendicular to the field direction. Thus cholesteric lc DNA aligns with its twist axis parallel to a sufficiently strong magnetic field.

Cholesteric lc DNA samples between slide and coverslip were placed in magnetic fields. The molecules orient parallel to glass interfaces, therefore the twist axis was generally perpendicular to the plane of the slide before placement in the magnetic field. A magnetic field **H** of one of four fixed strengths (1.1 T, 3.5 T, 6.3 T, 9.4 T) was then applied in the plane of the slide. Optical microscopy using crossed polarizers was employed to study the resulting textures. A 530 nm quarter wave plate was used to distinguish regions of opposite birefringence.

At sufficiently high magnetic field the twist axis reorients to be parallel to the field. At 1.1 T no reorientation is seen. At magnetic fields of 3.5 T and 6.3 T the twist axis aligns with the field. At 9.4 T a striped texture is observed. The reorientation of the twist axis corresponds to a degenerate Fréedericksz transition in cholesterics. The degeneracy arises from the two possible choices for reorientation parallel or antiparallel to the field. General summaries of Fréedericksz transitions in nematics are available in texts [8,9]. Meyer considered the unwinding of a positive diamagnetic anisotropy cholesteric in magnetic fields [10]. A number of re-

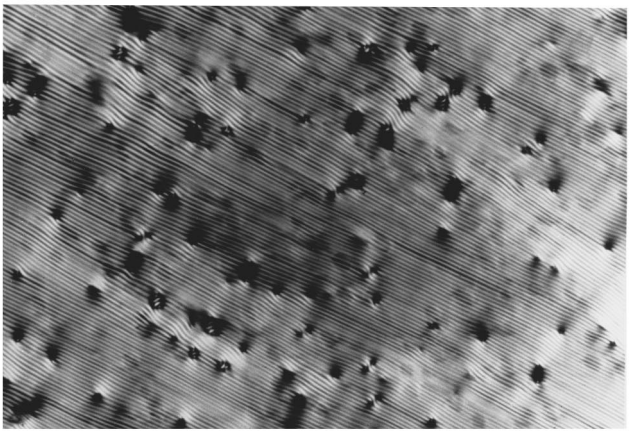

(a)

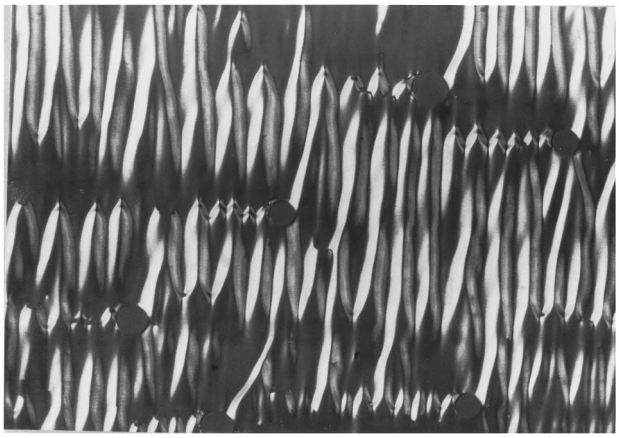

(b)

FIG. 1. (a) The fingerprint texture in lc DNA is shown. The magnetic field direction was perpendicular to the average orientation of the striations. (b) The striped texture observed in lc DNA in 9.4 T field under crossed polarizer and analyzer. The magnetic field direction was parallel to the average orientation of the stripes.

searchers further considered cholesterics in magnetic and electric fields [11–15]. The case of Fréedericksz transitions in polymer liquid crystals has been reviewed by Kini [16].

The size and axial ratio of the lc DNA under study (50 nm long and 3–5 nm in diameter) suggests that the elastic anisotropy, while larger than that of most thermotropics, is smaller than that of many polymer liquid crystals. Therefore the periodic distortions associated with large aspect ratio seen by Lonberg and Meyer [17] should not occur.

The primary features of the metastable textures observed in lc DNA are found upon numerically integrating the Euler-LaGrange equations obtained from the Frank elastic energy. This approach has been used by Berreman and Heffner to obtain metastable states in cholesterics under electric fields [11].

III. CALCULATION

In order to extract the essential physics resulting in the formation of stripe distortions a simplified model was developed. The coordinate system was chosen such that the sample lay in the x-z plane, with z indicating the direction of the magnetic field (see Fig. 2). The observed textures were assumed to be translationally invariant along the light path

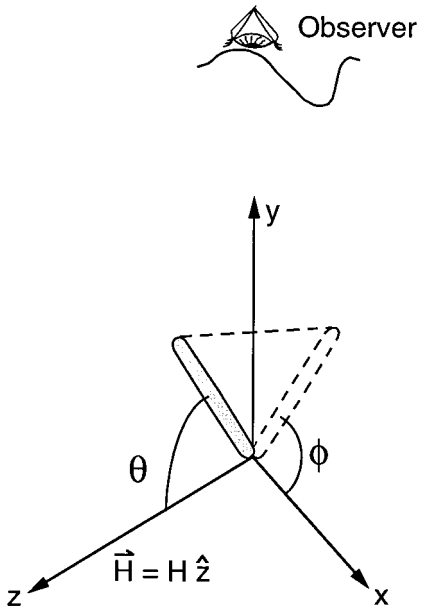

FIG. 2. The coordinate system used in the solutions of the ordinary differential equations.

(y axis) thereby reducing the problem to two dimensions. This assumption precludes simulating the defects [which are the points where bright and dark stripes merge in Fig. 1(b)].

When the system is treated as two dimensional in a plane parallel to the slide, solutions to the Euler-Lagrange equations

$$\frac{d}{dx}\left(\frac{\partial F}{(\partial\theta/\partial x)}\right)+\frac{d}{dz}\left(\frac{\partial F}{(\partial\theta/\partial z)}\right)-\frac{\partial F}{\partial\theta}=0 \tag{1}$$

and

$$\frac{d}{dx}\left(\frac{\partial F}{(\partial\phi/\partial x)}\right)+\frac{d}{dz}\left(\frac{\partial F}{(\partial\phi/\partial z)}\right)-\frac{\partial F}{\partial\phi}=0\,, \tag{2}$$

where F is the Frank elastic free energy, should describe the stable director configurations.

The Frank free energy for a cholesteric in the presence of a magnetic field is given by

$$F=\frac{K_1}{2}(\boldsymbol{\nabla}\cdot\mathbf{n})^2+\frac{K_2}{2}(\mathbf{n}\cdot\boldsymbol{\nabla}\times\mathbf{n}+q_0)^2+\frac{K_3}{2}(\mathbf{n}\times\boldsymbol{\nabla}\times\mathbf{n})^2 -\frac{1}{2}\chi_a(\mathbf{H}\cdot\mathbf{n})^2, \tag{3}$$

where K_1,K_2, and K_3 are the elastic constants for splay, twist and bend, respectively, q_0 is the intrinsic twist, χ_a is the diamagnetic anisotropy, and $\mathbf{H}$ is the magnetic field. The director $\mathbf{n}$ in Eq. (3) can be represented in spherical coordinates as

$$\begin{aligned} n_x&=\sin(\theta)\cos(\phi),\\ n_y&=\sin(\theta)\sin(\phi),\\ n_z&=\cos(\theta). \end{aligned} \tag{4}$$

Once derived, the differential equations (DEs) of Eqs. (1) and (2) were solved for two cases. In case 1, the variation of the director was considered only in the plane of the sample perpendicular to the field (along x). In case 2 the variation of the director was considered only parallel to the field direction (along z). The details of the derivations of the Euler-Lagrange equations for the two cases are included in the Appendix.

A. Numerical solutions

The DEs were integrated numerically using fourth order Runge-Kutta and Bullirsch-Stoer algorithms among others [18]. A variety of computational strategies were employed in order to test for and eliminate numerical artifacts associated with any one technique. All approaches led to essentially the same set of solutions. Unless otherwise stated the results reported were integrated using a fourth order Runge-Kutta algorithm.

In solving the DEs, the applied magnetic field, the intrinsic twist of the cholesteric and the elastic constants were all separately varied to explore the range of observable structures in parameter space. One thousand lattice sites were sampled. The field strength measured as $\alpha=\chi_a H^2/K_3$ (the inverse of the magnetic coherence length squared $\alpha=\xi^{-2}$) was varied from 0 to -10^{11} cm^{-2}. This corresponds to a range in ξ from infinity to a few hundredths of a micrometer. When solving in the x direction, the total distance covered by the simulation is an input parameter in cgs units. When solving in the z direction the intrinsic twist q_0, in units of radians per lattice spacing, was set to either 0, 0.01, or 0.02. Since the pitch is known from experiment, the choice of q_0 determines the length scale for those simulations. The one constant approximation ($K=K_1=K_2=K_3$) or the approximation $K_1/K_3=K_2/K_3=2$ with $K_3=1$ was used for elastic constants. The ratio of 2 attempts to account for typical values of elastic constants for macromolecular lyotropic liquid crystals [17]. The discussion that follows focuses on the distortions that can arise in the director for nonzero magnetic field. A uniform fingerprint texture is always obtained by setting the field to zero.

1. Case 1: θ and ϕ vary along x (perpendicular to H)

When the director was allowed to deviate from its equilibrium orientation, numerical solution showed that an oscillatory distortion of the director appears in the presence of magnetic fields. This is apparently the reason that the birefringent stripe texture forms. A series of numerical refinements were undertaken to try to understand why the stripe texture only forms at high fields and anneals away when removed from the field.

Solution of the Euler-Lagrange equations allowing θ and ϕ to vary freely resulted in oscillatory modes in both θ and ϕ (Fig. 3). While distortion from their equilibrium orientations occurred for $|\alpha|\geq 10$ cm^{-2}, the oscillations became evident for $|\alpha|\geq 400$ cm^{-2}. The solutions indicated that both ϕ and θ distort in a complicated way about the x and z axes, respectively, with increasing z coordinate. The actual observation, birefringent stripes superposed on a distorted fingerprint texture, corresponds to slight distortions in θ away from $\pi/2$ and variation in ϕ, about some average value.

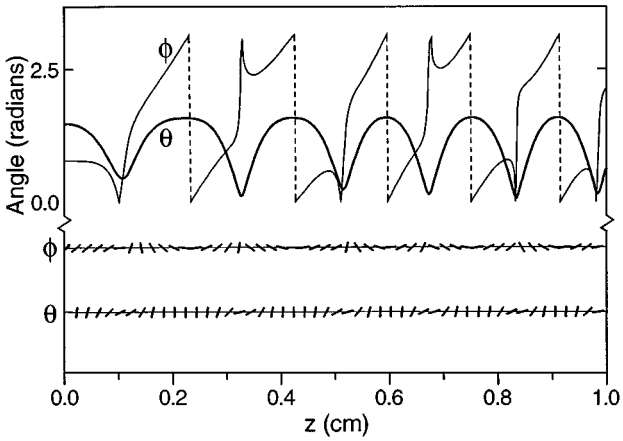

FIG. 3. (a) Solutions for θ and ϕ obtained by solving Eqs. (A5), (A6), thus allowing unconstrained director variation. Shown below the plots of θ and ϕ as a function of position are line segments oriented at the angles ϕ (measured from the x axis) and θ (measured from the z axis) plotted above the centers of the line segments. The calculation indicating that θ approaches zero is unphysical as this would orient the director parallel to the magnetic field. The large variation in ϕ when θ approaches zero is not completely unphysical, because the projection in the x-y plane is small there.

Thus allowing both θ and ϕ to vary freely resulted in solutions which were inconsistent with observation (for example, the DNA does not ever become parallel to the field axis, corresponding to $\theta=0$).

In order to test whether the oscillatory solution was an artifact of the integration technique used, the equations were solved again using the Bullirsch-Stoer algorithm. In principle, this algorithm gives better error correction than fourth order Runge-Kutta. Figure 4 shows a typical quasiperiodic oscillatory solution obtained. This confirms that the basic character of the oscillation is a general feature which appears when the Euler-LaGrange equations are solved simulta-

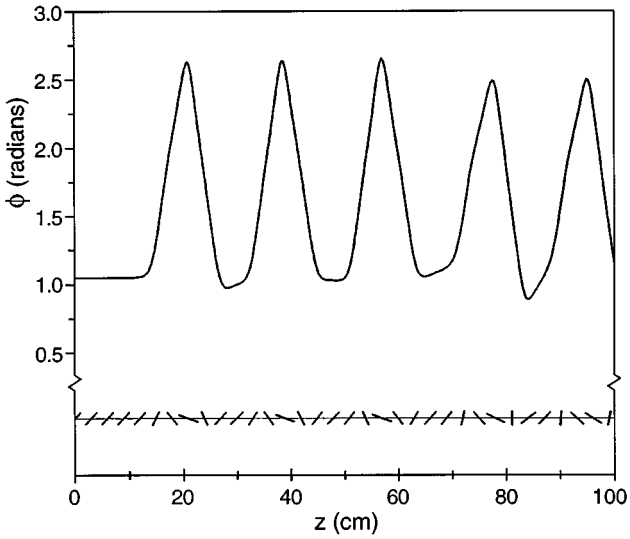

FIG. 4. Solution for ϕ using a Bullirsch-Stoer algorithm. Both equations for case 1 are solved simultaneously with $\alpha=40$. Shown below the plot of ϕ are line segments oriented at the angle given by the value of ϕ at the center of the line segment.

neously. Because the simultaneous solutions resulted in rotations of the director which seemed to be unphysical, simplifications were made to understand what aspects of the model retained the essential physics. That is, the oscillation in ϕ which appears in the solution is consistent with the observation of birefringent stripes appearing at high field. The question remained, can a physically reasonable solution be obtained preserving this oscillatory behavior of ϕ?

Allowing the integration schemes to freely distort the variables of integration resulted in θ approaching 0 repeatedly. One way of preventing θ from approaching 0 is to fix its value. By so fixing θ at a value slightly different from $\pi/2$, a splay-bend mode in ϕ was found. Typically, ϕ would oscillate about its minimum energy orientation. The amplitude and periodicity of this oscillation in ϕ depended on the tilt of θ away from $\pi/2$. In this case, the oscillation of ϕ is consistent with the observation of birefringence changing periodically. Unfortunately, the approximation that θ was constant is unphysical since it actually fluctuates about the equilibrium position because of thermal excitations.

In order to account for thermal excitations, the fluctuation spectrum near equilibrium was approximated by

$$\exp\left(\frac{-1}{2k_BT}(Kq^2-\chi_a H^2)(\delta\theta)^2\right), \tag{5}$$

where K is an average elastic constant, $\delta\theta$ is the angle out of the cholesteric plane, k_BT is the Boltzmann factor, and q is a wave vector associated with the spatial extent of the fluctuation. While bounds may be set on q, thermal fluctuations do exist on all length scales, consequently, the width of the Gaussian becomes an input parameter. Thus the spatial extent of the perturbation could be set by choices for α and $\sigma=\sqrt{k_BT/K(q^2-\alpha^2)}$, the standard deviation.

The Euler-Lagrange equations derived from Eq. (A4) were solved for ϕ [using Appendix Eqs. (A5) and (A6) and the variable transformation of Eq. (A2)]. For these solutions, α was fixed while $\delta\theta$ was treated as a Gaussian random variable [19] with σ, the width of the Gaussian, as an input parameter. Again, oscillatory solutions for ϕ were found. Typically, ϕ would oscillate about $\pi/2$ for several hundred lattice sites, and then jump to an oscillation about $3\pi/2$ or $-\pi/2$. The choice of α determined the periodicity of the oscillation. These solutions indicated that the orientation rotated without regard to neighbors in the z direction. Since unconstrained rotation is unphysical, one additional parameter was introduced.

A damping term which constrains next-nearest neighbor (on the 1000 site lattice) distortions was subtracted from the field induced change in orientation. This term is of the form $\beta\Delta\phi_{i-1,i-2}$, where β is a wave vector and $\Delta\phi_{i-1,i-2}=\phi_{i-2}-\phi_{i-1}$. The wave vector is not $2\pi/P$, where P is the periodicity of the stripes (that periodicity is selected by α), but is the local wave vector of the bend-splay distortion along x associated with the surfaces of uniform curvature. An undistorted cholesteric is characterized by planar surfaces of constant director orientation (the orientation twists perpendicular to the surfaces). The birefringent stripes are characterized by curved surfaces about which the director orientation twists. The angular change in orientation across a pair of stripes (in the x direction) is about $\pi/4$ rad, and the width of the pair is about 10 μm, thus the wave vector $\beta=2\pi/80\ \mu\text{m}^{-1}\approx 800\ \text{cm}^{-1}$. When all three parameters α, σ, and β are varied independently, a range of values for β between 400 and 2000 cm^{-1} is found to give reasonable solutions. When β is chosen based on the measurement of the curvature ($\beta = 800\ \text{cm}^{-1}$) then α and thus the average elastic constant can be determined.

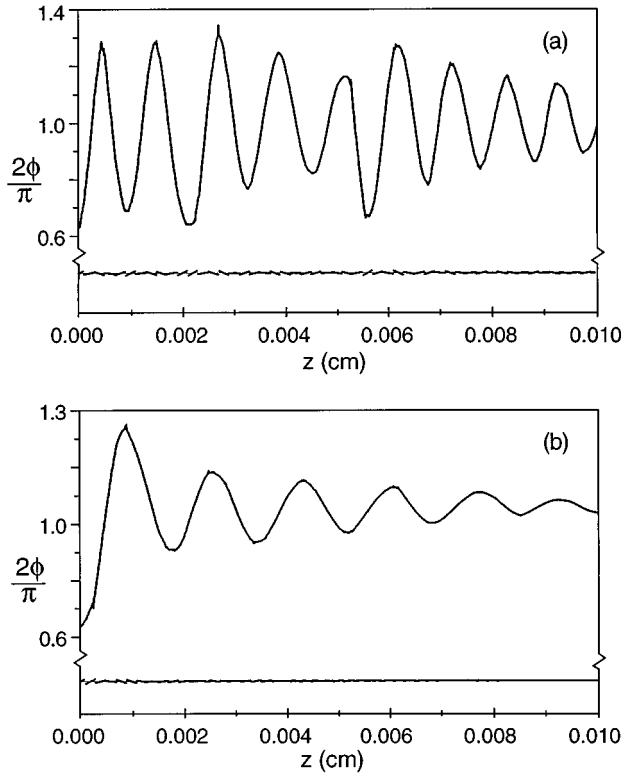

FIG. 5. Two solutions for $2\phi/\pi$ in case 1 representing the magnetic field stabilized oscillation (a) and the solution where the magnetic field is insufficient to overcome damping (b). In this case the tilt out of the plane perpendicular to the magnetic field is treated as a random variable (leading to the jaggedness of the data). Data for the parameters $\beta=800\ \text{cm}^{-1}$ and for (a) $\alpha=\chi_a H^2/K=2.5\times10^9\ \text{cm}^{-2}$ and for (b) $\alpha=1\times10^9\ \text{cm}^{-2}$ are shown. These show the essential features of the solution to case 1. For the larger value of α the oscillation is stable and has the correct $\sim$10 μm period. For the smaller α the period is larger than that observed in the sample and the oscillation decays away in a short distance, thus stripes are not expected to be observed.

Typical results of these simulations are shown in Fig. 5. Notable features of those data include an oscillation of ϕ about $\pi/2$, an exponentially decaying envelope about the oscillation when α is too small, and a small amplitude random noise term superposed on the oscillatory distortion of ϕ. The oscillation is not observed at all if the director is forced to remain in the cholesteric plane ($\theta=\pi/2$), while it is observed whenever the director is allowed to tilt out of the cholesteric plane. To treat this result in a physically reasonable way, the out of plane director orientation was treated as a fluctuating random variable. The small amplitude noise term superposed on the ϕ versus x plots is an artifact of the variable transformation of Eq. (A2) from the coordinate system used in the integration to that being used here.

2. Case 2: θ and ϕ vary along z (parallel to H

Integration of the Euler-Lagrange equations in the z direction resulted in a perfectly constant pitch when θ was held constant at $\pi/2$. However, allowing θ to vary away from this equilibrium value showed that ϕ was no longer a linear function of z. Thus, $d\phi_2/dz = q(z)$ was no longer a constant. The usual fingerprint texture became distorted due to the presence of an additional splay-bend mode. This occurred for all α including $\alpha = 0$. A long wavelength distortion of this type may be observed in the lc DNA system.

Solution of case 1 shows that θ fluctuates about its equilibrium value in the presence of a magnetic field. Solution of case 2 shows that, in the presence of such fluctuations, a constant pitch cholesteric is not expected. Even in the absence of a magnetic field, the pitch varies. This distortion is associated with thermal fluctuations. Damping of this distortion was not included in the model since divergent solutions were not observed.

IV. DISCUSSION

A. Birefringent stripes: Case 1

Low density cholesteric lc DNA placed in a 9.4 T field exhibits birefringent stripes which are oriented parallel to the field direction. Their formation is now understood to be an oscillation in the director orientation stabilized by the magnetic field. In addition, the wavelength of the oscillation is shown to be a function of magnetic field. Solutions to the appropriate Euler-Lagrange equation are calculated by evolving ϕ versus position. The basic character of the oscillatory solutions is seen in Fig. 5. Plotted are $2\phi/\pi$ versus x for two parameter sets. Also shown are a series of line segments representing the projection of the director orientation in the x-y plane at the position determined by the center of the line segment. The special value of $\phi = \pi/2$ (corresponding to 1.0 on the vertical axis) is an arbitrary phase included in the variable choice for the Frank free energy in Eq. (A4). This phase changes continuously along the z direction representing the twist of the cholesteric director. When ϕ became larger than π or smaller than zero, numerically, the oscillations occurred about $3\pi/2$ or equivalently $-\pi/2$. These modes were the same as those about $\pi/2$ since the director is not a vector. By increasing the scale along the x axis, oscillatory solutions with a few peaks in the calculated range are found for much smaller values of α and/or σ. Thus the simulation predicts an oscillatory distortion, the spatial frequency of which depends on α.

The cgs system of units is chosen to apply to the simulation and to the experimental data. For the real DNA system, alignment of the twist axis occurs at $|\mathbf{H}| \leqslant 35$ kG. The anisotropy in magnetic susceptibility is 4.5×10^{-8} emu cm^3/G [from superconducting quantum interference device (SQUID) magnetometer measurements] [20]. Typically the average elastic constants for polymer liquid crystals are on the order of 5×10^{-7} dyn. For these values the magnetic coherence length would be ~ 0.9 μm. When the oscillatory distortion manifests itself at larger fields (94 kG), the coherence length (assuming the same parameters) would be $\sim 0.3\mu$m. In performing the simulation, we are able to extract a range of values for the average orientational elastic constants.

For the data shown in Fig. 5, both sets have 1000 equally spaced points in x from 0 to 0.01 cm. The initial value of θ was chosen as 1 rad, and the initial slope chosen as 1 rad/cm. For both data sets σ was chosen to be 0.15. For Fig. 5(a) $\alpha = 2.5\times10^9$ cm^{-2} (therefore the magnetic coherence length $\xi = 0.2$ μm) while for Fig. 5(b) $\alpha = 1.0\times10^9$ cm^{-2} ($\xi = 0.32$ μm). In both cases ξ is short enough that the system consisting of a 10 μm thick sample should undergo the Fréederickz transition to align the twist axis with the field.

The simulations, in addition to justifying the presence of distortions perpendicular to the field direction, provided information regarding the allowed values for the elastic constants. The experimental observations were that no oscillatory behavior of ϕ was seen for 3.5 or 6.4 T fields, while birefringent stripes with spacing ~ 10 μm was seen for an applied field of 9.4 T. The physically reasonable values of α and σ resulting in that periodicity are limited. To get a 10 μm spacing from the oscillation with $\alpha = 10^9$ cm^{-2}, σ must be ~ 0.25. This corresponds to a very large fluctuation in orientation out of perpendicular to the aligning field. For $\alpha = 2.5, 5$, and 10×10^9 cm^{-2}, respectively, σ must be 0.15, 0.11, and 0.07 to give the correct periodicity. For those values of α the coherence length ranges from $\xi = 0.2$ to 0.1 μm. Thus the reasonable range in the value of the average elastic constant $K = \chi_a H^2/\alpha$ is $K = 4\times10^{-7}$ for $\alpha = 10^9$ to $K = 4\times10^{-8}$ for $\alpha = 10^{10}$. This range compares well with measurements by others on rodlike polymer liquid crystals [17,21]. When the choice of β is made based on the measurement of the curvature observed in the lc DNA system $\beta = 800$ cm^{-1} then $\alpha = 2.5\times10^9$ cm$^{-2} \pm 1\times10^9$ cm^{-2} for stable solutions.

In the physical system, at 9.4 T the birefringent stripes only occur in the lower density cholesteric regions. In some samples, a concentration gradient existed with birefringent stripes in the low density cholesteric bounded by higher density aligned fingerprint texture with no stripes, bounded by the higher density columnar phase [2]. The phase transition from cholesteric to columnar requires that K_1 and K_2 increase and ultimately diverge just prior to the transition [22]. When the elastic constants increase, α will decrease, the length scale for the oscillatory distortion in ϕ will increase, and any oscillation will decay within a short distance [as in Fig. 5(b)] and will not be observed.

B. Distortions of fingerprint: Case 2

Solving the Euler-Lagrange equations in the direction parallel to the magnetic field revealed the presence of a nonconstant pitch. This variation in pitch was not related to the increase in pitch seen in positive diamagnetic anisotropy materials as the magnetic field unwinds the twisted structure. For the negative diamagnetic anisotropy materials being considered here, in the absence of distortions, the twist axis will align parallel to the field direction and no spatial variation or field dependent change in pitch is expected. Observation of all cholesteric fingerprint textures which were obtained by alignment in 3.5 and 6.4 T fields showed pitch variations parallel to the field direction. These variations were typically discounted as being due to surface defects or inhomogeneities, but apparently are associated with near equilibrium perturbations about the minimum energy state.

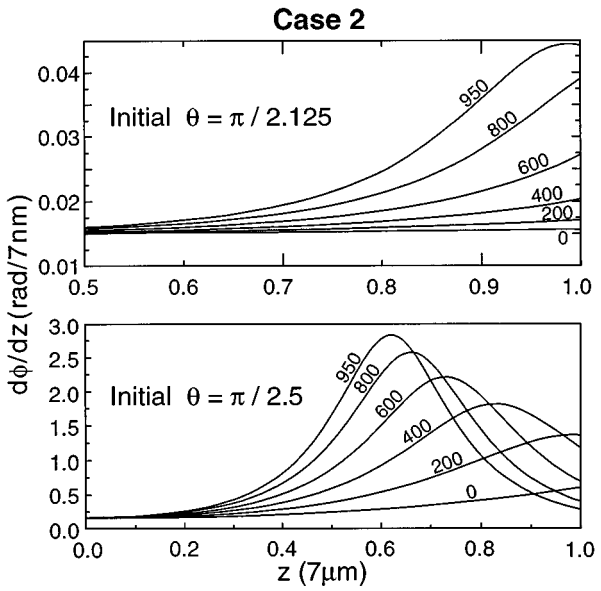

FIG. 6. Plots showing the derivative of ϕ with respect to z as a function of z for case 2. The distance scale along z is determined by the intrinsic twist per lattice site (0.02 rad). Field amplitudes range from 1 to 950. These values are divided by that distance scale (7×10^{-4} cm) squared to compare with α used for case 1. (a) The initial value of θ is $\pi/2.125$. (b) The initial value of θ is $\pi/2.5$.

The length scale for case 2 is determined based on the number of lattice sites (1000) and the chosen average twist per site. Since the DNA cholesteric pitch is 2.2 μm [7] the choice of twist per site (typically 0.02 rad) determines the length scale simulated. For a 1000 site lattice, at 0.2 rad/site and a pitch of 2.2 μm, the lattice size corresponds to 7.0 μm. Thus the α's used in case 2, correspond to the α's in case 1 by a multiplicative factor of 49×10^{-8}. The pitch $q=d\phi/dz$ as a function of lattice site is plotted in Fig. 6. The individual graphs in Fig. 6 are distinguished by the fixed tilt of θ away from $\pi/2$. For small values of $|\theta-\pi/2|$ and small α, the variation in pitch was small [Fig. 6(a), $\alpha=100$]. As α was increased a very long wavelength periodicity in the pitch became evident.

C. Summary

Cholesteric lc DNA is a novel polymer liquid crystalline system for a variety of reasons. This paper focuses on some consequences of its negative diamagnetic anisotropy. When placed in a magnetic field, a Frèedericksz transition occurs, causing the twist axis to align (on average) parallel to the magnetic field. By integrating the Euler-Lagrange equations derived from the orientational Frank free energy, distortions to the perfect fingerprint texture have been found in agreement with experimental observation of the lc DNA system. The disorientation arises when the projection of the director in the direction of the magnetic field is nonzero. That is, when there exists a net torque on the molecules.

In simulating the observed lc DNA textures, the two directions in the plane of a confined sample were treated separately for simplicity. The details of the derivations in each case are outlined in the Appendix. The treatment of the two directions separately led to underdamped and divergent solutions for some ranges of the parameters. This was corrected for in case 1 by including a next-nearest neighbor term in the DEs which represented long-range interactions. Damping in case 2 was not necessary since divergent solutions were not present for physically meaningful parameters.

The periodicity of the birefringent stripes shown in Fig. 1(b) is obtained by treating the spherical angles θ and ϕ as a function only of the distortion axis x (case 1). An oscillatory distortion arises as an instability due to the presence of fluctuations in molecular orientation out of the plane perpendicular to the applied magnetic field. By solving the Euler-Lagrange equations derived from the Frank free energy, and incorporating measured values of the magnetic field and the diamagnetic anisotropy of DNA fragments, approximate values for the average Frank elastic constants were determined.

Solutions of the DEs along the field axis z indicated that pitch varies with position due to the fluctuations from perpendicular alignment. Distortions and fluctuations in both θ and ϕ always exist due to boundary conditions and thermal excitations. The deviation from the perfect cholesteric became more pronounced as the field strength was increased.

ACKNOWLEDGMENT

This research was supported by the State of Florida through the Center for Materials Research and Technology (Martech).

APPENDIX

1. Case 1: θ and ϕ as a function of x only (perpendicular to the field)

In order to obtain the simplest functional forms for the DEs the spherical-polar coordinate system is chosen such that the polar angle η is chosen from the x axis, and the azimuthal angle ζ is chosen in the y-z plane. With this choice of angles the director takes the form

$$n_x=\cos(\eta),$$
$$n_y=\sin(\eta)\cos(\zeta), \tag{A1}$$
$$n_z=\sin(\eta)\sin(\zeta).$$

Comparison with Eq. (4) reveals the η and ζ are related to θ and ϕ by

$$\cos(\eta)=\sin(\theta)\cos(\phi), \tag{A2}$$
$$\sin(\zeta)=\frac{\sin(\theta)\sin(\phi)}{\sin(\eta)}.$$

In the (η,ζ) coordinate system, a perfect cholesteric in a magnetic field given $\mathbf{H}=H\hat{z}$ with twist axis parallel to the field corresponds to $\zeta=0$, and η any value from $[0,2\pi]$. Near the $\zeta=0$ state, using Eqs. (A1), Eq. (4), and small angle approximations for the trigonometric functions, ϕ and θ are related by

$$\phi\sim\frac{\eta}{\sqrt{2}}, \tag{A3}$$

$$\theta \sim \sqrt{2(1-\eta\zeta)}.$$

Since a well defined cholesteric corresponds to the regime $\zeta \to 0$, the physically relevent solutions for the lc DNA system allow for a one-to-one correspondence between ϕ and η.

Substitution of Eq. (A1) into the Frank free energy of Eq. (3) gives

$$F = \tfrac{1}{2}\{K_1\ \eta'^2 \sin^2(\eta) + K_2\ \zeta'^2 \sin^4(\eta) + K_3 \cos^2(\eta) \times [\ \eta'^2 + \ \zeta'^2 \sin^2(\eta)] - \chi_a H^2 \sin^2(\eta)\cos^2(\zeta)\}. \tag{A4}$$

The notation a' implies da/dx and a'' means d^2a/dx^2. Note that the the intrinsic twist term has been dropped. This reflects the fact that since the twist axis is assumed to be parallel to $\hat{z}$ we expect no intrinsic twist along x. Further, variations in the z direction are not considered.

The resulting Euler-Lagrange equation for the polar angle η is

$$\eta'' = \{(K_3 - K_1)\ \eta'^2 + \ \zeta'^2[2K_2 \sin^2(\eta) + K_3 \cos(2\eta)] - \chi_a H^2 \cos^2(\zeta)\} \frac{\sin(2\eta)}{2[K_1 \sin^2(\eta) + K_3 \cos^2(\eta)]}. \tag{A5}$$

The equation for the azimuthal angle ζ is

$$\zeta'' = \frac{-\ \eta'\ \zeta'[2K_2 \sin^2(\eta) + K_3 \cos(2\eta)]\sin(2\eta)}{\sin^2(\eta)[K_2 \sin^2(\eta) + K_3 \cos^2(\eta)]} + \frac{\chi_a H^2 \sin(2\zeta)}{2[K_2 \sin^2(\eta) + K_3 \cos^2(\eta)]}. \tag{A6}$$

We note that fixed points of the DEs arise for $\eta = n\pi/2$ and $\zeta = n\pi/2$ for any integer n since this causes the sines to vanish in the numerator of each equation. These values correspond to states of stable or unstable equilibrium and can be chosen to be any value with a suitable choice for the phase (i.e., a suitable coordinate rotation).

2. Case 2: θ and ϕ as functions of z only (parallel to the field)

In this case the simplest equations are obtained by using the coordinates mentioned in Eq. (4), $n_x = \sin(\theta)\cos(\phi)$, $n_y = \sin(\theta)\sin(\phi)$, and $n_z = \cos(\theta)$. The same prescription outlined in case 1 is followed. Differentiation with respect to z only is carried out. The intrinsic pitch is included since, along the z direction, by construction we expect the cholesteric twist to be nonzero. Substitution of Eq. (4) into Eq. (3) leads to

$$F = \tfrac{1}{2}\{K_1\ \theta'^2 \sin^2(\theta) + K_2[\ \phi' \sin^2(\theta) - q_0]^2 + K_3 \cos^2(\theta) \times [\ \theta'^2 + \ \phi'^2 \sin^2(\theta)] - \chi_a H^2 \cos^2(\theta)\}. \tag{A7}$$

The resulting Euler-Lagrange equation for θ is

$$\theta'' = [(K_3 - K_1)\ \theta'^2 + 2K_2\ \phi'(\ \phi' \sin^2(\theta) - q_0) + K_3\ \phi'^2 \cos(2\theta) + \chi_a H^2] \frac{\sin(2\theta)}{2[K_1 \sin^2(\theta) + K_3 \cos^2(\theta)]}. \tag{A8}$$

The equation for ϕ in this case is

$$\phi' = \frac{K_2 q_0 + C/\sin^2(\theta)}{K_2 \sin^2(\theta) + K_3 \cos^2(\theta)}, \tag{A9}$$

where C is an integration constant associated with intrinsic twist (set to values of 0.0, 0.01, and 0.02 rad per unit lattice spacing for different runs). Since Eq. (A9) does not contain H, the dependence of ϕ on the field arises only implicitly through the field dependence of θ. Further we also note that $\theta = n\pi$ for any integer n (corresponding to the director oriented parallel to the field) leads to a singularity in Eq. (A9).

[1] D. H. Van Winkle, M. W. Davidson, and R. L. Rill, in *Physical Phenomena at High Magnetic Fields Proceedings 1991*, edited by E. Manousakis, P. Schlottmann, P. Kumar, K. S. Bedell, and F. M. Mueller (Addison-Wesley, Redwood City, CA, 1992), p. 469.

[2] D. H. Van Winkle, A. Chatterjee, R. Link, and R. L. Rill, preceding paper, Phys. Rev. E **55**, 4354 (1997).

[3] Y. Bouligand, J. Microsc. (Paris) **17**, 145 (1973).

[4] T. E. Strzelecka, M. W. Davidson, and R. L. Rill, Nature (London) **331**, 457 (1988).

[5] J. A. Schellman and D. Stitger, Biopolymers **16**, 1415 (1977).

[6] D. Stitger, Biopolymers **16**, 1435 (1977).

[7] D. H. Van Winkle, M. W. Davidson, W. X. Chen, and R. L. Rill, Macromolecules **23**, 4140 (1990).

[8] S. Chandrasekar, *Liquid Crystals* (Cambridge University Press, New York, 1992).

[9] P. G. deGennes, *Physics of Liquid Crystals*, Oxford University Press, Oxford (1974).

[10] R. B. Meyer, Appl. Phys. Lett. **12**, 281 (1968).

[11] D. W. Berreman and W. R. Heffner, J. Appl. Phys. **54**, 3032 (1981).

[12] J. Rault, C. R. Acad. Sci. **272**, 1275 (1971).

[13] W. Helfrich, Appl. Phys. Lett. **17**, 531 (1970); J. Chem. Phys. **55**, 839 (1971).

[14] J. P. Hurault, J. Chem. Phys. **59**, 2068 (1973).

[15] F. M. Leslie, Mol. Cryst. Liq. Cryst. **12**, 57 (1970).

[16] U. D. Kini, Mol. Cryst. Liq. Cryst. **153**, 1 (1987).

[17] F. Lonberg and R. B. Meyer, Phys. Rev. Lett. **55**, 6 (1985).

[18] W. H. Press, S. A. Teukolsky, W. T. Vetterling, and B. P. Flannery, *Numerical Recipes in C: The Art of Scientific Programming* (Cambridge University Press, New York, 1992).

[19] S. E. Koonin, *Computational Physics* (Benjamin Cummings, Menlo Park, CA, 1986), p. 195.

[20] T. P. Szabo, D. H. Van Winkle, J. Dharia, Y. J. Liu, R. L. Rill, and B. R. Locke, in *Proceedings of Physical Phenomena at High Magnetic Fields II*, edited by Z. Fisk, L. Gor'kov, D. Meltzer, and R. Schrieffer (World Scientific, Singapore, 1996), p. 743.

[21] V. G. Taratuta, A. J. Hurd, and R. B. Meyer, Phys. Rev. Lett. **55**, 246 (1985).

[22] A. Chatterjee and D. H. Van Winkle, Phys. Rev. E **49**, 1450 (1994).